Pergamon

J. Mech. Phys. Solids, Vol. 46, No. 2, pp. 291–311, 1998

Printed in Great Britain
0022-5096/98 $19.00+0.00

PII: S0022-5096(97)00062-8

SWITCH-TOUGHENING OF FERROELECTRICS SUBJECTED TO ELECTRIC FIELDS

W. YANG and T. ZHU

Department of Engineering Mechanics, Tsinghua University, Beijing 100084, China

(*Received* 11 *December* 1996; *in revised form* 26 *August* 1997)

ABSTRACT

Electric fields can influence the fracture toughness of ferroelectrics. For example, poled ferroelectrics exhibit fracture toughness anisotropy: the material is tougher for a crack parallel to the poling direction but less tough for a crack perpendicular to it. When an electric field is applied to a poled sample, a positive field reduces its fracture toughness but a negative field enhances it. Previous investigations attribute these phenomena to polarization switching. This paper proposes a model of stress-assisted 90° polarization switching to quantify the toughening process. Small scale switching and uniform electric fields are assumed. An analytical solution is presented for a mono-domain ferroelectric crystal undergoing a confined polarization switch. This solution and the domain orientation pattern enable us to estimate the fracture resistance against the steady state crack growth in ferroelectrics by a Reuss-type multiple-domain assembly. A dimensionless group of material parameters and an electric field function emerge, and form the key ingredients of switch-toughening. The model is used to delineate several observations, including: poling-induced anisotropy of the fracture toughness, asymmetric variation of the fracture toughness under positive and negative electric fields of a poled specimen; upside-down butterfly loop for the fracture toughness response under cyclic electric loading.

Keywords: A. electromechanical processes, A. fracture toughness, B. ferro-electric material, switch-toughening.

1. INTRODUCTION

Increasing use of ferroelectric ceramics in smart structures, such as sensors and actuators, raises the important issue of their reliability; see Winzer *et al.* (1989), and Uchino (1993). Crack-like defects were observed in multilayer actuators (Furuta and Uchino, 1993; Cao and Evans, 1994), and analyzed for cracking from a conductive electrode and an impermeable crack; see Suo (1993), Yang and Suo (1994), Lynch *et al.* (1995) and Hao *et al.* (1995). These analyses only addressed the effect of incompatible strain induced by non-uniform electric field. The toughening mechanism of ferroelectrics by progressive polarization switching has barely been touched.

Polarization switching assigns a unique feature of ferroelectrics. A switching of 180° causes little strain, and is activated primarily by the electric field, whereas a switching of 90° results from the electric and stress fields. It delivers a sizable strain of fixed amount and orientation, contracting along the previous polarization direction, and elongating along the current one.

The fracture toughness data of ferroelectric ceramics motivate a link between the

toughening mechanism and the polarization switch assisted by the crack tip stress. It has been established, through Vicker's indentation technique, that the measured fracture toughness for cracks propagating along the poling direction and the ones normal to it are different. The former has a shorter crack length upon indentation, and consequently higher fracture toughness; and the latter has a longer crack length and lower fracture toughness; see Yamamoto *et al.* (1983), Okazaki (1984), Pisarenko *et al.* (1985), Virkar and Matsumoto (1986), Mehta and Virkar (1990), Virkar *et al.* (1991), Tobin and Pak (1993), Singh and Wang (1995) and Lynch (1995). Recent consensus attributes the fracture toughness anisotropy to polarization switching, but few mechanistic models have been proposed. The existing models, many of which have appeared in the Russian literature (see a review of Kramarov and Rez (1991)), do not recognize the importance of the switching wake.

Another group of experimental observations involve the *asymmetric* variation of fracture toughness of poled ferroelectrics under positive and negative electric fields. A positive field directs along the poling axis while a negative field against it. The apparent fracture toughness is measured either from Vicker's indentation (Tobin and Pak, 1993), or from a compact tension specimen (Park and Sun, 1995). The data showed that the fracture toughness declines continuously as the positive field increases, but increases when a negative electric field is imposed.

The present paper aims at quantifying the toughening mechanism of ferroelectrics by 90° polarization switching. A framework of switch-toughening is sketched in the next section. A dimensionless group of material parameters emerges to scale the extent of toughening. Section 3 provides an analytical solution for a mono-domain ferroelectric crystal toughened by small scale polarization switch. By this solution and the domain distribution pattern under a prescribed electric field, we propose in Section 4 a Reuss-type multiple-domain assembly to estimate the fracture resistance against steady state crack growth in ferroelectrics. The analysis leads to an electric field function (which involves both the poling and the applied fields) to quantify the switch-toughening. Section 5 applies the model to two cases for which experimental data are available. The present model quantitatively predicts the fracture toughness anisotropy after poling. It explains the asymmetric variation of fracture toughness of poled ferroelectrics under positive and negative electric fields. Under cyclic electric loading, the present analysis predicts an upside-down butterfly loop between the fracture toughness and the electric field.

2. SWITCH-TOUGHENING

Scales of switching

If the influence of residual stress is ignored, the apparent fracture toughness of ferroelectric ceramics mainly comes from two contributions: the intrinsic fracture toughness (denoted as $K_{\text{intrinsic}}$) due to the creation of material surfaces, and the toughening due to polarization switch. The extent of switching classifies different toughening regimes. Global switching is irrelevant to the presence of defects. It changes the distribution of domain orientations, but offers no direct contribution to

the toughening. Large scale switching refers to a large switching zone size, comparable to the specimen characteristic length. Its mechanistic modeling is complicated and part of the switching effect is lost by insufficient constraint. Attention here will be focused on the case of *small scale switching*, in the sense that the specimen size is considerably larger than the switching zone size. In small scale switching, all switching strains induced by the crack tip stress concentration cannot be accommodated by global deformation, and serve to toughen the material.

Switching criteria

Polarization switch occurs when a switching criterion is satisfied. Here we adopt the switching criteria used by Hwang *et al.* (1995). A switching of 180° is irrelevant of stresses, and activated if

$$E_i \Delta P_i \geqslant 2P_s E_c \tag{1}$$

where E_i and ΔP_i are the electric field and the polarization switch vectors, P_s the magnitude of spontaneous polarization, and E_c the coercive field. The right hand side of eqn (1) describes a threshold energy for polarization switch, and this threshold energy will remain constant for all polarization switches induced by electric and mechanical fields.

In the absence of stresses, the criterion (1) also applies to the uniform 90° switching of ferroelectrics. In the presence of electric and mechanical fields, a 90° switch is activated by the combined work

$$\sigma_{ij} \Delta \varepsilon_{ij} + E_i \Delta P_i \geqslant 2P_s E_c \tag{2}$$

where σ_{ij} is the stress tensor, and $\Delta \varepsilon_{ij}$ the switching strain tensor. The latter is scaled by ε_c such that $\Delta \varepsilon_{ij} = \varepsilon_c \tilde{\varepsilon}_{ij}$. The quantity ε_c is a certain fraction of the crystallographic estimate $(c-a)/a_0$. The energy criterion eqn (2) is equivalent to the following "stress type" criterion for polarization switch:

$$\sigma_{ij} \tilde{\varepsilon}_{ij} \geqslant \frac{P_s E_c}{\varepsilon_c} \left(2 - \frac{E_i}{E_c} \frac{\Delta P_i}{P_s} \right) \equiv \sigma_c, \tag{3}$$

namely switching occurs if the stress combination $\sigma_{ij} \tilde{\varepsilon}_{ij}$ reaches a critical stress σ_c.

Switch-toughening

Two basic assumptions are adopted in this paper: (1) the stress-assisted switching zone is confined within the specimen; and (2) the electric field is uniform. The first assumption requires that the electric field is weaker than either the poling field, or the field for a global 90° switching. The second assumption overlooks the perturbation on the electric field by the presence of defects. It is admissible for the case of a conducting crack, and is also valid for contacting or shallow cracks, as in the case of Vicker's indentation. Toughness variation under the non-uniform electric field is different from the present analysis, see Zhu and Yang (1997).

Switch-toughening can be pursued in the spirit of transformation-toughening in ceramics; see McMeeking and Evans (1982), Budiansky *et al.* (1983) and Lam-

bropoulos (1986). The criterion eqn (3) can be viewed as a stress criterion of "transformation". According to the transformation-toughening theory, a transformation wake shields the crack tip stress intensity factor by the following amount

$$\Delta K = -\alpha \frac{Y\varepsilon_c}{1-\nu^2}\sqrt{H}, \tag{4}$$

where Y denotes the Young's modulus, ν the Poisson's ratio, and H the characteristic height of the wake. The constant α in eqn (4) does not depend on material parameters.

For the case of small scale switching, the stress field near the switching boundary may be approximated by the remote K field

$$\sigma_{ij} = \frac{K^{\infty}}{\sqrt{2\pi r}}\Sigma_{ij}(\theta) \tag{5}$$

where r and θ are polar coordinates focused at the crack tip. A remote mode I loading is considered here. Accordingly, K^{∞} is the mode I applied stress intensity factor and $\Sigma_{ij}(\theta)$ the corresponding universal angular distribution function. The remote field approximation similar to eqn (5) was adopted by McMeeking and Evans (1982) for the case of transformation-toughening of ceramics. The accuracy of that approximation was justified by the full field calculation of Budiansky *et al.* (1983), provided the transformation zone is small.

The combination of eqns (3) and (5) suggests a scaling law for the switching zone size

$$\sqrt{H} \propto \frac{K^{\infty}}{\sigma_c}. \tag{6}$$

Substituting eqn (6) and the expression of σ_c into eqn (4), one derives the following dimensional form for the shielding ratio $\Delta K/K^{\infty}$

$$\Delta K/K^{\infty} = -\eta\Omega. \tag{7}$$

The shielding effect by polarization switch is scaled by a key dimensionless group of material parameters

$$\eta = \frac{Y\varepsilon_c^2}{(1-\nu^2)P_s E_c}. \tag{8}$$

Two interpretations exist for this dimensionless parameter: (1) it measures the ratio between the elastic strain energy and the energy threshold for switching; and (2) it measures the ratio between the elastic stress caused by a plane strain switching $Y\varepsilon_c/(1-\nu^2)$, and the "yield stress", $\sigma_c \propto P_s E_c/\varepsilon_c$, against the switching. The η values range from 5 to 20 for typical ferroelectric ceramics.

The function Ω in eqn (7) depends on the electric field and the domain orientation of the specimen. We term this function the electric field function. Switch-toughening can be influenced by the electric field from two aspects. The poling electric field may re-configure the pre-test domain orientations of ferroelectrics, and consequently change its polarization switching during the toughness testing. On the other hand,

the electric field applied to the specimen during a toughness test would shift the barrier for the stress-assisted 90° switching.

Evaluation of the electric field function depends on the model details. We will pursue this evaluation in the subsequent sections, starting with the simple case of mono-domain ferroelectrics.

3. MONO-DOMAIN SOLUTION

Mono-domain ferroelectrics

We first consider the simple case of mono-domain ferroelectrics, such as single crystal ferroelectrics under uniform poling. The discussion is restricted to the in-plane mechanical and electric fields. Coordinates X_1 and X_2 are introduced, such that X_1 is along the crack direction and X_2 is normal to it. The mono-domain ferroelectrics has a uniform initial poling direction, which forms an angle ϕ with the X_1 axis. Within a region surrounding a growing crack tip, 90° switching occurs under the assistance of crack tip stress, resulting in toughening. This section will provide an analytical solution for the plane strain mono-domain toughening. Apart from its own merit, the solution may provide a basis to estimate the toughening of multiple-domain ferroelectrics, as will be illustrated in Section 4 by using a Reuss approximation.

A electric field of strength E and direction ω is imposed on the mono-domain ferroelectric crystal. From the switching criterion eqn (1), 180° switching cannot occur when $E < E_c$; when $E > E_c$, it occurs if

$$|\phi - \omega| \geqslant \pi - \cos^{-1}\frac{E_c}{E} \equiv \phi_{180}. \tag{9}$$

A 180° switching in a mono-domain crystal does not cause mechanical fields.

In the absence of stresses, the criterion eqn (1) also applies to the global 90° switching of mono-domain ferroelectric crystals. When $E < \sqrt{2}E_c$, 90° switching cannot occur; when $E \geqslant \sqrt{2}E_c$, 90° switching occurs if

$$|\phi - \omega| \geqslant \frac{\pi}{4} + \sin^{-1}\frac{\sqrt{2}E_c}{E} \equiv \phi_{90}. \tag{10}$$

Between the two variants of 90° switching, the one with less $|\phi - \omega|$ value (or the one with higher algebraic value of the electric work $E_i\Delta P_i$) would prevail. In eqns (9) and (10), we choose that both ϕ and ω range from 0 to π.

In the presence of electric and mechanical fields, a 90° switching occurs when the criterion eqn (2) is satisfied. The switching strain tensor is constant throughout the switching zone, and given by

$$\varepsilon_{ij} = \varepsilon_c \begin{bmatrix} -\cos 2\phi & \sin 2\phi \\ \sin 2\phi & \cos 2\phi \end{bmatrix}. \tag{11}$$

The second work product on the left hand side of eqn (2) assumes different values for positive and negative 90° variants. The actual switching selects the variant with higher

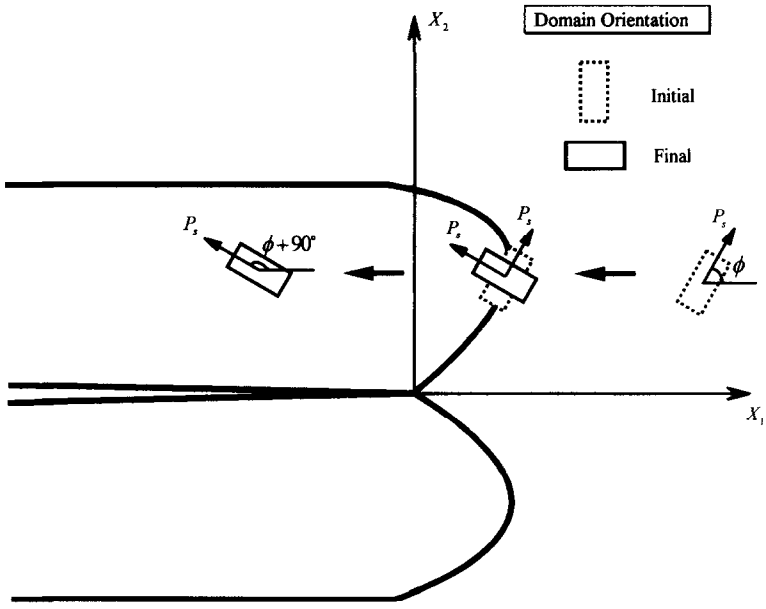

Fig. 1. Schematics of the 90° polarization switching in a mono-domain ferroelectric crystal activated by the stress concentration near a growing crack tip.

algebraic value of that work term. Substituting eqn (11), the electric field and the polarization switching field into the stress criterion eqn (3) of switching, one obtains

$$\frac{\sigma_{22}-\sigma_{11}}{2}\cos 2\phi+\sigma_{12}\sin 2\phi \geqslant \frac{P_s E_c}{\varepsilon_c}\left(1-\frac{E}{\sqrt{2}E_c}A(\phi-\omega)\right)\equiv \sigma_c(\phi) \tag{12}$$

where

$$A(\phi-\omega)=\max\begin{cases}\cos\left(\phi-\omega\pm\dfrac{3\pi}{4}\right) & \text{if } |\phi-\omega|<\phi_{180}\\ -\cos\left(\phi-\omega\pm\dfrac{3\pi}{4}\right) & \text{if } |\phi-\omega|>\phi_{180}\end{cases} \tag{13}$$

The applied electric field only affects the stress threshold for the switching.

Geometry of the switching zone

Stress concentration near a crack tip produces a confined switching zone. If the reverse switching is neglected, a growing crack would result in switching strips as shown in Fig. 1. It is asymmetric with respect to the crack except when $\phi = 0, \pi/2, \pi$. For a given material particle below the maximum height of the switching zone, a 90° switching occurs when the particle is swept by the frontal switching boundary. The geometry of the switching zone can be estimated by substituting the remote K field

approximation eqn (5) into eqn (12). The radius of the switching zone, denoted by R, relates to the polar angle θ by

$$R = \frac{1}{8\pi}\left\{\frac{K^{\infty}}{\sigma_c(\phi)}\right\}^2 \sin^2\theta \sin^2\left(2\phi + \frac{3}{2}\theta\right), \tag{14}$$

where $\sigma_c(\phi)$ is defined in eqn (12). The electric field alters only the size, but not the shape, of the switching zone. Equation (14) is valid only if $\sin\theta \sin(2\phi + 3\theta/2) > 0$, which furnishes the initial angles, denoted as θ_i^+ and θ_i^-, for polarization switchings above and below the crack extension line,

$$\theta_i^+ = \begin{cases} 0 & 0 \leqslant \phi \leqslant 3\pi/8 \\ 4(\pi - \phi)/3 & 3\pi/8 < \phi \leqslant \pi \end{cases}; \quad \theta_i^- = \begin{cases} -4\phi/3 & 0 \leqslant \phi \leqslant 5\pi/8 \\ 0 & 5\pi/8 < \phi \leqslant \pi \end{cases}. \tag{15}$$

The terminating angles θ_f^+ and θ_f^- refer to the polar angles where the maximum heights of the switching zones above and below the crack are reached. They are determined as

$$\theta_f^+ = \begin{cases} \frac{2}{5}(\pi - 2\phi) & 0 \leqslant \phi \leqslant 3\pi/8 \\ \frac{2}{5}(3\pi - 2\phi) & 3\pi/8 < \phi \leqslant \pi \end{cases}; \quad \theta_f^- = \begin{cases} -\frac{2}{5}(\pi + 2\phi) & 0 \leqslant \phi \leqslant 5\pi/8 \\ \frac{2}{5}(\pi - 2\phi) & 5\pi/8 < \phi \leqslant \pi \end{cases}. \tag{16}$$

The ranges between the initial angles and the terminating ones describe the angle spans of the frontal switching boundary.

For a growing crack, the frontal switching boundary translates as the crack advances, while the rear switching boundary remains immobile. Two strips of switching zones are stretched above and below the crack, whose heights, H^+ and H^-, are

$$H^{\pm} = \pm\frac{1}{8\pi}\left(\frac{K^{\infty}}{\sigma_c(\phi)}\right)^2 (\sin\theta_f^{\pm})^5. \tag{17}$$

For some occasions, say ϕ between $3\pi/8$ and $\pi/2$, a secondary frontal wake may form. One may verify that this small perturbation has no effect in the subsequent calculations.

For the case of dilatant transformation, it was shown by McMeeking and Evans (1982) that the toughening effect of the transformed region approaches the steady state limit (namely a wake of infinite length) when the crack growth amount Δl exceeds twice the size of the wake height. In the transformation-toughening involving both dilatant and shear contributions, rapid converging to the steady state asymptote is anticipated; see Lambropoulos (1986). For the present case of polarization switching, we will estimate the upper bound of the toughening effect. The switching zone geometry in a mono-domain ferroelectric crystal is depicted in Fig. 2, where $E = 0$ and $\phi = 0$, $\pi/4$, $\pi/2$. The switching zones above and below the crack are symmetric when the domain direction is either parallel or normal to the crack, and are asymmetric

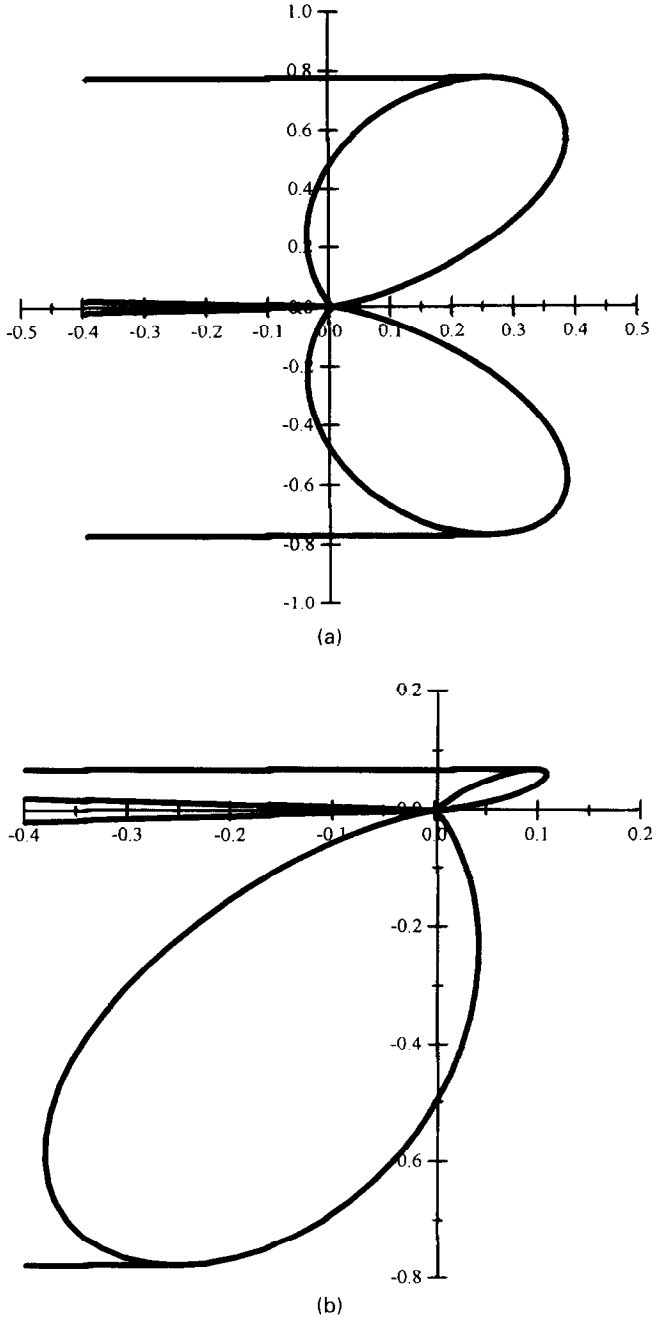

Fig. 2. Geometry of the switching zones in a mono-domain ferroelectric crystal, $E = 0$, $\phi = 0, \pi/4, \pi/2$.

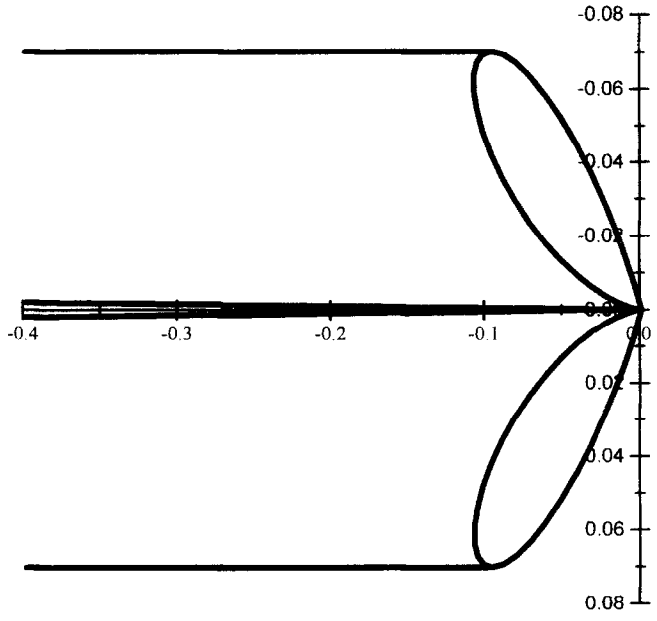

(c)

Fig. 2—*continued.*

otherwise. The size of the switching zone is large when the polarization direction is parallel to the crack, and small when the polarization direction is normal to the crack.

Switching induced toughening

The analysis for the switching zone can be formulated by an Eshelby technique; see Eshelby (1957) and McMeeking and Evans (1982). The zone has a shape described by eqns (14) to (17) and undergoes a uniform switching strain eqn (11). The switching strain induces a thin layer of accommodating body force T_i on the boundary Γ_s of the switching zone. Since the switching strain is deviatoric, one has

$$T_i = \frac{Y}{1+\nu}\Delta\varepsilon_{ij}n_j, \tag{18}$$

where n_j denotes the outward normal of Γ_s. We assume that the crack extends straight ahead and is dictated by the mode I stress intensity factor. The toughness increment is evaluated by

$$\Delta K = \oint_{\Gamma_s} T_i h_i \, d\Gamma, \tag{19}$$

where h_i is the mode I stress intensity factor by a unit body force along X_i direction applied at a point (r, θ) to the crack geometry. Substituting eqns (18) and (11) into eqn (19), one has

$$\Delta K = \frac{Y\varepsilon_c}{1+\nu}\left\{\cos 2\phi \oint_{\Gamma_s} (n_2 h_2 - n_1 h_1)\,d\Gamma + \sin 2\phi \oint_{\Gamma_s} (n_1 h_2 + n_2 h_1)\,d\Gamma\right\}. \tag{20}$$

The case of small scale switching admits the geometry of a semi-infinite crack in an otherwise infinite medium, leading to

$$\begin{Bmatrix} h_1 \\ h_2 \end{Bmatrix} = \frac{1}{2(1-\nu)\sqrt{2\pi r}} \begin{Bmatrix} \cos\theta/2(2\nu - 1 + \sin\theta/2 \sin 3\theta/2) \\ \sin\theta/2(2 - 2\nu - \cos\theta/2 \cos 3\theta/2 \end{Bmatrix}. \tag{21}$$

Substitutions of eqn (21) and the switching zone geometry (eqns (14) to (17)) into eqn (20) lead to the exact evaluation of the toughness increments. This procedure is outlined in Appendix A. The result is

$$\Delta K(\phi) = -\eta \frac{F(\phi)}{2 - \dfrac{\sqrt{2}E}{E_c} A(\phi - \omega)} K^{\infty}, \tag{22}$$

where the dimensionless material parameter group η is given by eqn (8). The function $F(\phi)$ in eqn (22) characterizes a toughening function for domain orientation. It obeys the following periodicity relations

$$F(\phi) = F(-\phi) = F(\pi - \phi) = F(2k\pi + \phi) \quad k: \text{integers}. \tag{23}$$

In a typical range from 0 to $\pi/2$, a closed form solution of F is

$$F(\phi) = \frac{5}{32\pi}\left(\sin\frac{\pi}{5}\cos\frac{12\phi}{5} + 2\sin\frac{2\pi}{5}\cos\frac{4\phi}{5}\right), \quad 0 \leqslant \phi < \frac{3\pi}{8}$$

$$F(\phi) = \frac{5}{32\pi}\left(2\sin\frac{\pi}{5}\cos\frac{2\pi + 4\phi}{5} + \sin\frac{2\pi}{5}\cos\frac{\pi - 12\phi}{5}\right), \quad \frac{3\pi}{8} < \phi \leqslant \frac{\pi}{2}. \tag{24}$$

The function $F(\phi)$ is plotted in Fig. 3. The largest value occurs when the domain direction is parallel to the crack, since a horizontal domain is easily switched to a "standing up" orientation by the crack tip stress field. The toughening function $F(\phi)$ declines continuously as ϕ increases and reaches the minimum point at $\phi = \pi/2$. It is difficult to switch a vertical domain to a "lying down" orientation by the crack tip stress field. Representative values of $F(\phi)$ are:

$$F(0) = \frac{5}{32\pi}\left(\sin\frac{\pi}{5} + 2\sin\frac{2\pi}{5}\right) \approx 0.1238,$$

$$F(\pi/4) = \frac{5}{64\pi}\left(3\sin\frac{\pi}{5} + \sin\frac{2\pi}{5}\right) \approx 0.0675,$$

$$F(\pi/2) = \frac{5}{32\pi}\left(2\sin\frac{\pi}{5} - \sin\frac{2\pi}{5}\right) \approx 0.0112. \tag{25}$$

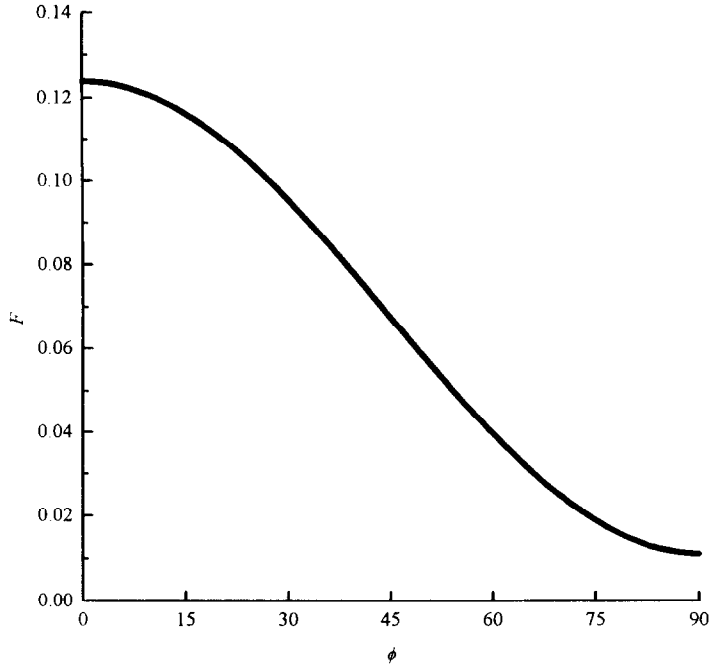

Fig. 3. Variation of toughening factor F vs domain orientation ϕ for a mono-domain ferroelectric crystal.

4. MULTIPLE-DOMAIN ESTIMATE ON TOUGHENING

Poling configuration

We next consider the ferroelectrics consisting of domains in different orientations. The orientation distribution function for a ferroelectric polycrystal is denoted by $f(\phi)$, which is normalized by

$$\int_{-\pi}^{\pi} f(\phi)\,\mathrm{d}\phi = 1. \tag{26}$$

Poling on an initially ferroelectric polycrystal re-configures its domain orientation distribution. Suppose that the poling field has a strength E_0 and a direction ω_0. In the absence of mechanical stresses, no polarization switch would occur if $E_0 < E_c$. When $E_c \leqslant E_0 < \sqrt{2}E_c$, a switching of 180° occurs for the domains whose orientations satisfy eqn (9). When $E_0 \geqslant \sqrt{2}E_c$, a switching of 90° occurs if eqn (10) is satisfied. In summary, we have

$$f(\phi) = \frac{1}{2\pi} \qquad \text{if } E_0 < E_c$$

$$f(\phi) = \frac{1}{2\pi}\begin{cases} 2 & |\phi-\omega_0| < \pi-\phi_{180} \\ 1 & \text{if } \pi-\phi_{180} \leqslant |\phi-\omega_0| < \phi_{180} \\ 0 & |\phi-\omega_0| \geqslant \phi_{180} \end{cases} \qquad \text{if } E_c \leqslant E_0 < \sqrt{2}E_c$$

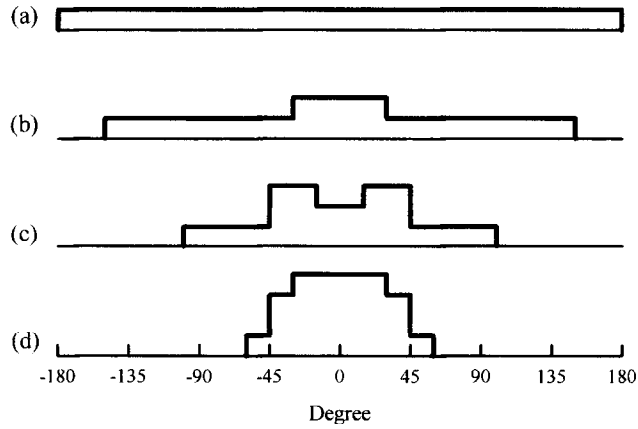

Fig. 4. Orientation distribution functions for various poling strengths. From top to bottom: (a) $E_0 < E_c$; (b) $E_c \leqslant E_0 < \sqrt{2}E_c$; (c) $\sqrt{2}E_c \leqslant E_0 < 2E_c$; (d) $E_0 \geqslant 2E_c$.

$$f(\phi) = \frac{1}{2\pi}\begin{cases} 2 & |\phi-\omega_0| \leqslant \phi_{90}-\pi/2 \\ 3 & \phi_{90}-\pi/2 \leqslant |\phi-\omega_0| < \pi/4 \\ 1 & \pi/4 \leqslant |\phi-\omega_0| < \phi_{90} \\ 0 & |\phi-\omega_0| \geqslant \phi_{90} \end{cases} \text{if } \sqrt{2}E_c \leqslant E_0 < 2E_c$$

$$f(\phi) = \frac{1}{2\pi}\begin{cases} 4 & |\phi-\omega_0| \leqslant \pi/2-\phi_{90} \\ 3 & \pi/2-\phi_{90} \leqslant |\phi-\omega_0| < \pi/4 \\ 1 & \pi/4 \leqslant |\phi-\omega_0| < \phi_{90} \\ 0 & |\phi-\omega_0| \geqslant \phi_{90} \end{cases} \text{if } E_0 \geqslant 2E_c. \quad (27)$$

Figure 4 depicts the orientation distribution function for various poling strengths. Fully poled ferroelectrics refer to the case that f equals to $2/\pi$ for $|\phi-\omega_0| \leqslant \pi/4$ and vanishes elsewhere.

Reuss approximation

We now assemble the mono-domain solution and the poling configuration for a multiple-domain representation of ferroelectrics. A Reuss type approximation (Hill, 1963) is used for this estimate. Consider a continuum element in a multiple domain ferroelectric aggregate. The size of this element is small when comparing to the macroscopic length scales, but large when comparing to the domain size. Prior to the stress activated 90° switching, the element contains domains whose polarization directions are configured by the orientation function eqn (27). The Reuss approximation assumes that all domains in that element are subjected to the same macroscopic stresses and the same electric field; see Hwang *et al.* (1995). Their fates of switching are determined by the criterion eqn (2) which relates to their individual orientations. Different switching strains occur for different domain orientations in this continuum

element. We assume, as in all Reuss-type assembly, that different switching strains are accommodated without appreciable local interaction. The remote K field is used to estimate the stress for all domain orientations and for all continuum elements where stress activated polarization switching may occur. Proceeded as such, the collective toughening effect is composed of an integration over all orientations for a specific continuum element and a further area integral over all (partially and fully switched) continuum elements in the entire switching zone. Since the domain orientation distributions are the same for all continuum elements, one can change the order of integrations. The area integral will be carried out first, giving rise to a contribution of $\Delta K(\phi) f(\phi)\,\mathrm{d}\phi$ for all domains in the switching zone with orientations between ϕ and $\phi+\mathrm{d}\phi$. Further integration with respect to all domain orientations leads to the following superposition integral:

$$\Delta K = \int_{-\pi}^{\pi} \Delta K(\phi) f(\phi)\,\mathrm{d}\phi = -\eta\Omega\left(\frac{E}{E_c}, \frac{E_0}{E_c}, \omega, \omega_0\right) K^{\infty}. \tag{28}$$

Please notice the resemblance between eqns (28) and (7). The electric field function Ω is now specified as

$$\Omega\left(\frac{E}{E_c}, \frac{E_0}{E_c}, \omega, \omega_0\right) = \int_{-\pi}^{\pi} \frac{F(\phi)}{2 - \dfrac{\sqrt{2}E}{E_c} A(\phi-\omega)} f(\phi-\omega_0, E_0/E_c)\,\mathrm{d}\phi \tag{29}$$

under a Reuss approximation. It will be evaluated for several practical cases in Section 5.

The near tip stress intensity factor, K_{tip}, is the sum of the applied stress intensity factor and the shielding by ΔK,

$$K_{tip} = K^{\infty} + \Delta K = K^{\infty}(1-\eta\Omega). \tag{30}$$

K_{tip} should sustain at the value of $K_{intrinsic}$ during the crack propagation. Thus, an apparent fracture resistance against steady state crack growth K_{ss} is given by

$$K_{ss} = \frac{K_{intrinsic}}{1-\eta\Omega}. \tag{31}$$

In eqn (31), the influence of material parameters on toughening is characterized by the η value defined in eqn (8) and the influence due to poling and applied electric fields is characterized by the electric field function Ω defined in eqn (29). A locking on crack growth would be predicted if

$$\eta\Omega \geqslant 1. \tag{32}$$

Unconstrained switching and limitations

The preceding Reuss approximation implies an unconstrained switching of a domain in a continuum element, provided that the macroscopic stress and electric fields satisfy the 90° switching criterion eqn (2). This approximation may lead to an erroneous prediction when the electric field is near or beyond the level of a global 90

switching. From eqns (13) and (14), a mono-domain under such a critical condition would have a switching zone of an infinite size, violating the small scale switch assumption. Furthermore, the integral expression (29) for the electric field function would have a singular end point of Cauchy's type when the electric field is near or beyond the level of a global 90° switching. Consequently, a small spectrum of domains (which switch without constraint for a large scale) would dominate the toughening response of the aggregate. This amplification for poorly represented domains breaks down the Reuss approximation. The present solution can only be used for the case when the applied electric field is considerably lower than either the poling field, or the global 90° switching field for the unpoled ferroelectrics. Possible extensions to the case of constrained switch will be discussed in Section 6.

5. APPLICATIONS

Anisotropy in fracture toughness of poled ferroelectrics

We will illustrate two applications of the present model, through evaluating the electric field function Ω for each case. Attention is first focused on the fracture toughness testing of poled ferroelectrics, while the applied electric field is absent. The extent of poling is given by the domain orientation distribution eqn (27). The simplified formula for Ω in this case is

$$\Omega = \Omega(E_0/E_c, \omega_0) = \frac{1}{2}\int_0^{\pi} [F(\phi+\omega_0)+F(\phi+\omega_0]f(\phi, E_0/E_c)\,d\phi. \tag{33}$$

If the poling field strength is below the level of global 90° switching, or $E_0 < \sqrt{2}E_c$, poling will have little effect on the toughness. The explicit result for this case is

$$\Omega = \frac{1}{2\pi}\int_0^{\pi} F(\phi)\,d\phi = \frac{25}{384\pi^2}\left(6\sin\frac{2\pi}{5} - \sin\frac{\pi}{5}\right) \approx 0.0338. \tag{34}$$

When $E_0 \geqslant \sqrt{2}E_c$, 90° switching occurs in the process of poling. Substitution of eqn (27) into eqn (33) leads to

$$\Omega = \frac{1}{4\pi}\left(\int_0^{\phi_{90}} + \int_0^{\pi/4} + \int_{\phi_{90}-\pi/2}^{\pi/4}\right)[F(\phi+\omega_0)+F(\phi-\omega_0)]\,d\phi \quad \text{if } \sqrt{2}E_c \leqslant E_0 < 2E_c$$

$$\Omega = \frac{1}{4\pi}\left(\int_0^{\phi_{90}} + 2\int_0^{\pi/4} + \int_0^{\pi/2-\phi_{90}}\right)[F(\phi+\omega_0)+F(\phi-\omega_0)]\,d\phi \quad \text{if } E_0 \geqslant 2E_c. \tag{35}$$

For the special case of 45° poling, it is straightforward to show that eqn (34) is recovered regardless of the intensity of poling, namely

$$\Omega(E_0/E_c, \pi/4) \approx 0.0338. \tag{36}$$

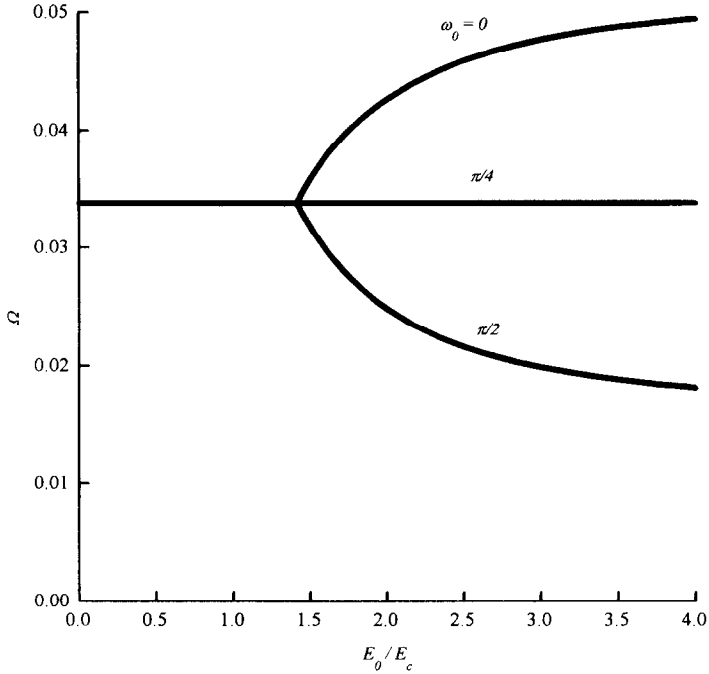

Fig. 5. Curves of the electric field function Ω vs the poling field strength E_0/E_c, $E = 0$. The representative poling angles are $\omega_0 = 0, \pi/4, \pi/2$.

We plot in Fig. 5 the Ω vs E_0/E_c curves for three poling angles, $\omega_0 = 0, \pi/4, \pi/2$. All three curves have the same Ω value of 0.0338 when $E_0 \leqslant \sqrt{2}E_c$, and become distinct when $E_0 > \sqrt{2}E_c$. As the poling intensifies, a crack perpendicular to the poling direction embrittles; a crack parallel to the poling direction toughens; and the toughness for a crack in a specimen poling by 45° remains constant. This prediction on the anisotropy of fracture toughness explains all relevant experimental data; see Yamamoto *et al.* (1983), Okazaki (1984), Pisarenko *et al.* (1985), Virkar and Matsumoto (1986), Mehta and Virkar (1990), Virkar *et al.* (1991), Tobin and Pak (1993), Singh and Wang (1995) and Lynch (1995).

Fracture toughness of fully poled ferroelectrics tested under positive and negative fields

We next consider the fracture toughness tests under combined mechanical and electrical loadings, but the specimen is fully poled to justify the small scale switching assumption. This case will serve to explain the asymmetric variation of fracture toughness under positive and negative electric fields. For fully poled ferroelectrics, the expression eqn (29) is reduced to

$$\Omega = \Omega(E/E_c, \omega, \omega_0) = \frac{2}{\pi}\int_{\omega_0-\pi/4}^{\omega_0+\pi/4} \frac{F(\phi)}{2-\dfrac{\sqrt{2}E}{E_c}A(\phi-\omega)}\,\mathrm{d}\phi, \tag{37}$$

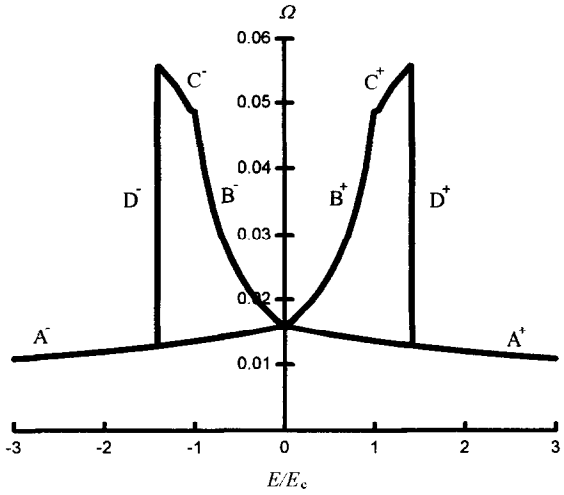

Fig. 6. Variation of the electric field function Ω under positive and negative electric fields. The ferroelectric ceramics is fully poled. An upside-down butterfly loop is revealed for cyclic electric loading.

where the function $A(\phi-\omega)$ is given by eqn (13). Consider the poling direction normal to the crack, namely $\omega_0 = \pi/2$. The applied electric field is assumed to be either positive ($\omega = \pi/2$) or negative ($\omega = -\pi/2$). For the positive electric loading, eqn (37) is reduced to

$$\Omega(E/E_c, \pi/4, \pi/4) = \frac{4}{\pi}\int_0^{\pi/4} \frac{F\left(\frac{\pi}{2}-\phi\right)\mathrm{d}\phi}{2+\frac{\sqrt{2E}}{E_c}\cos\left(\phi+\frac{\pi}{4}\right)}. \tag{38}$$

The Ω vs E/E_c curve describes the segment A^+ in Fig. 6. As the strength of the applied positive field increases, the fracture toughness declines continuously, which is in agreement with the test data by Tobin and Pak (1993), and by Park and Sun (1995) for positive field loading.

The case of negative field loading is twisted by the possibility of 180° switchings. When $0 < E < E_c$, the electric field function Ω is given by

$$\Omega(E/E_c, \pi/4, -\pi/4) = \frac{4}{\pi}\int_0^{\pi/4} \frac{F\left(\frac{\pi}{2}-\phi\right)\mathrm{d}\phi}{2-\frac{\sqrt{2E}}{E_c}\cos\left(\phi-\frac{\pi}{4}\right)}. \tag{39}$$

The corresponding Ω vs E/E_c curve is shown in Fig. 6 as the segment B^-. The curve indicates further increase of the fracture toughness as negative electric field is imposed, giving rise to an asymmetric fracture toughness variation. This prediction again agrees with the test data of Tobin and Pak (1993), and of Park and Sun (1995). If the negative

field falls within $E_c < E < \sqrt{2}E_c$, partial 180° switching occurs prior to the stress assisted 90° switching, then formula (39) should be replaced by

$$\Omega(E/E_c, \pi/4, -\pi/4) = \frac{4}{\pi}\left\{\int_0^{\pi-\phi_{180}} \frac{F\left(\frac{\pi}{2}-\phi\right)d\phi}{2+\frac{\sqrt{2}E}{E_c}\cos\left(\phi+\frac{\pi}{4}\right)} + \int_{\pi-\phi_{180}}^{\pi/4} \frac{F\left(\frac{\pi}{2}-\phi\right)d\phi}{2-\frac{\sqrt{2}E}{E_c}\cos\left(\phi-\frac{\pi}{4}\right)}\right\}. \quad (40)$$

Caution has to be exercised to use eqn (40) near $E = \sqrt{2}E_c$, where the small scale switching assumption is not valid for the domains with directions close to $\pi/4$, and the Reuss approximation is doomed. In fact, the second integral in eqn (40) does not vanish when $E \to \sqrt{2}E_c$, but rather approaches a constant value of $F(\pi/4)/2 \approx 0.034$. As shown in the curve segment C^- of Fig. 6, the electric field function keeps rising as the negative field intensifies. When the negative field surpasses $\sqrt{2}E_c$, the 180° switching is complete before the stress activated 90° switching, and the situation reverses to the case of positive electric field. A sudden drop of Ω (vertical line D^-) appears at $E = \sqrt{2}E_c$. After the drop, the fracture toughness decreases mildly as the negative field intensifies further, as shown in the lower-left segment A^- in Fig. 6.

We next consider the imposition of a cyclic electric field. By carefully examining the role of the 180° switching, one can construct an electric field function vs applied electric field (algebraic value) curve shown as the complete graph of Fig. 6, where segments A^-, B^+, C^+, D^+ are mirror reflections of segments A^+, B^-, C^-, D^-. This relationship predicts an upside-down butterfly loop between the fracture toughness and the applied electric field, provided the fracture toughness could be measured continuously during the cycling of the electric field.

6. CONCLUDING REMARKS

The present analysis reveals two governing factors of switch-toughening: the dimensionless material parameter group η and the electric field function Ω. The former measures the ratio between the elastic strain energy and the energy barrier of polarization switching, and the latter measures the effect of poling and applied electric fields. Further research is necessary to quantify these two factors. The term ε_c in the expression for η needs clarification. Due to the formation of twin domain bands of low energy, as well as the three dimensional nature of polarization switchings, ε_c is only a fraction of the uniform shear switching strain from the crystallographic calculation $(c-a)/a_0$. The electric field function Ω is evaluated in the present analysis under small scale switching and Reuss approximation. There are cases where the accommodated switching strains of individual domains lead to appreciable local constraining stresses.

This local stress field would modify the energy barrier for the 90° switching. When the applied electric field approaches or exceeds $\sqrt{2}E_c$, a small fraction of domain orientations near the critical state can switch in a large scale if the constraining effect by the neighboring non-switchable domains is overlooked, resulting in a dubious domination in the toughening effect by these critical domain orientations. To remedy this situation, a self consistent model outlined below may be worthy of further investigation. At a continuum element, the macroscopic strain is the average of the strains from various domain orientations. The difference between the strain of a particular domain orientation (after switching) and this macroscopic strain would cause local accommodation stress. This local stress can be calculated as the inclusion stress of a particle undergoing a transformation strain (Eshelby, 1957), and it has to be included in the switching criterion. A modified version of eqn (2) then determines the occurrence of polarization switching under constraint. This approach requires detailed calculations on continuum strain at various points, and is less tractable than the Reuss approximation.

Work is needed to extend the present switch-toughening model to deal with several intricate issues. One issue is mixed mode fracture, and the crack deflection resulting from it. Such a cracking mode was observed experimentally by McHenry and Koepke (1983). Another issue is the effect of a non-uniform electric field that may develop around the crack tip. Toughness variation under the non-uniform electric field is different from that under the uniform one. Furthermore, the influence of electric field is rather sensitive to the modeling of flaw boundary conditions; see Zhu and Yang (1997).

ACKNOWLEDGEMENTS

The work of W. Yang was supported by a visiting appointment at the University of California, Santa Barbara, funded by NSF through grant MSS-9258115, and by the National Natural Science Foundation of China. Stimulating discussions with Z. Suo of UCSB were essential in the development of this work. The authors appreciate the help of Mr Honghui Yu in preparing the figures of this paper.

REFERENCES

Budiansky, B., Hutchinson, J. W. and Lambropoulos, J. C. (1983) Continuum theory of dilatant transformation toughening in ceramics. *Int. J. Solids Structs.* **19,** 337–355.

Cao, H. C. and Evans, A. G. (1994) Electric-field-induced fatigue crack growth in piezoelectrics. *J. Amer. Ceram. Soc.* **77,** 1783–1786.

Eshelby, J. D. (1957) Determination of the elastic field of an ellipsoidal inclusion and related problems. *Proc. Roy. Soc. London, Ser. A* **241,** 376–396.

Furuta, A. and Uchino, K. (1993) Dynamic observation on crack propagation in piezoelectric multilayer actuators. *J. Amer. Ceram. Soc.* **76,** 1615–1617.

Hao, T. H., Gong, X. and Suo, Z. (1995) Fracture mechanics for the design of ceramic multilayer actuators. *J. Mech. Phys. Solids* **44,** 23–48.

Hill, R. (1963) Elastic properties of reinforced solids: some theoretical principles. *J. Mech. Phys. Solids* **11,** 357–372.

Hwang, S. C., Lynch, C. S. and McMeeking, R. M. (1995) Ferroelectric/ferroelastic interactions and a polarization switching model. *Acta Metall. Mater.* **43,** 2073–2084.
Kramarov, S. O. and Rez, J. S. (1991) Mechanical strength of ferroelectric single crystals and ceramics: experimental studies and fracture theory. *Prog. Crystal Growth and Charact.* **22,** 199–244.
Lambropoulos, J. C. (1986) Shear, shape and orientation effects in transformation toughening. *Int. J. Solids Structs.* **22,** 1083–1106.
Lynch, C. S. (1995) Fracture of ferroelectric and relaxor electro-ceramics: influence of electric field. Manuscripts in preparation.
Lynch, C. S., Yang, W., Collier, L., Suo, Z. and McMeeking, R. M. (1995) Electric field induced cracking in ferroelectric ceramics. *Ferroelectrics* **166,** 11–30.
McHenry, K. D. and Koepke, B. G. (1983) Electric field effects on subcritical crack growth in PZT. *Fract. Mech., Ceram.* **5,** 337–352.
McMeeking, R. M. and Evans, A. G. (1982) Mechanics of transformation-toughening in brittle materials. *J. Amer. Ceramic Soc.* **65,** 242–246.
Mehta, K. and Virkar, A. V. (1990) Fracture mechanisms in ferroelastic–ferroelastic lead zirconate titanate (Zr : Ti = 0.54 : 0.46) ceramics. *J. Amer. Ceramic Soc.* **73,** 567–574.
Okazaki, K. (1984) Mechanical behavior of ferroelectric ceramics. *Bull. Amer. Ceram. Soc.* **63,** 1150–1157.
Park, S. and Sun, C.-T. (1995) Fracture criteria for piezoelectric ceramics. *J. Amer. Ceram. Soc.* **78,** 1475–1480.
Pisarenko, G. G., Chushko, V. M. and Kovalev, S. P. (1985) Anisotropy of fracture toughness of piezoelectric ceramics. *J. Amer. Ceramic Soc.* **68,** 259–265.
Singh, R. N. and Wang, H. (1995) Crack propagation in piezoelectric materials under combined mechanical and electrical loadings: an experimental study. Proc. of AMD-Vol. 206/MD-Vol. 58, *Adaptive Materials Systems*, ed. G. P. Carman, C. Lynch and N. R. Sottos. ASME, 85–95.
Suo, Z. (1993) Models for breakdown-resistant dielectric and ferroelectric ceramics. *J. Mech. Phys. Solids* **41,** 1155–1176.
Tobin, A. G. and Pak, Y. E. (1993) Effects of electric field on fracture of piezoelectric ceramics. *Proc. SPIE, Smart Struct. Mater.* **1916,** 78–86.
Uchino, K. (1993) Ceramic actuators: principle and applications. *MRS Bulletin*, April Issue, 42–48.
Virkar, A. V. and Matsumoto, R. L. K. (1986) Ferroelastic domain switching as a toughening mechanism in tetragonal zirconia. *J. Am. Ceram. Soc.* **69,** C244–C226.
Virkar, A. V., Jue, J. F., Smith, P., Mehta, K. and Prettyman, K. (1991) The role of ferroelasticity in toughening of brittle materials. *Phase Transitions* **35,** 27–46.
Winzer, S. R., Shankar, N. and Ritter, A. P. (1989) Designing cofired multilayer electrostrictive actuators for reliability. *J. Am. Ceram. Soc.* **72,** 2246–2257.
Yamamoto, T., Igarashi, H. and Okazaki, K. (1983) Internal stress anisotropies induced by electric field in lanthanum modified $PbTiO_3$ ceramics. *Ferroelectrics* **50,** 273–278.
Yang, W. and Suo, Z. (1994) Cracking in ceramic actuators caused by electrostriction. *J. Mech. Phys. Solids* **42,** 649–663.
Zhu, T. and Yang, W. (1997) Toughness variation of ferroelectrics by polarization switch under non-uniform electric field. *Acta Mater.*, in press.

APPENDIX A: TOUGHENING CALCULATION FOR STEADY STATE CRACK GROWTH IN MONO-DOMAIN FERROELECTRICS

We divide the boundary of switching zone Γ_s (given by eqns (14) to (17)) into three segments: the crack surfaces; the top and bottom wake boundaries; and the frontal switching boundary.

The contribution from the crack surfaces is easy to calculate. Both the upper and the lower crack surfaces have the same toughening contribution, and the combination effect is

$$\Delta K^{(1)} = -2\sqrt{\frac{2}{\pi}}\frac{Y\varepsilon_c}{1+\nu}\cos 2\phi \tag{A1}$$

where Δl is the amount of crack growth.

The evaluation along the top and the bottom wake boundaries will be discussed next. First consider the top wake boundary, where we have

$$n_1 = 0, \quad n_2 = 1, \quad \frac{d\Gamma}{\sqrt{R}} = \sqrt{H^+}\frac{d\theta}{(\sin\theta)^{3/2}}. \tag{A2}$$

Substituting eqns (A2) and (21) into eqn (20) and integrating, we arrive at

$$\Delta K_+^{(2)} = \frac{Y\varepsilon_c\sqrt{H^+}}{2\sqrt{2\pi}(1+\nu)}\left[\frac{\cos\left(2\phi-\frac{\alpha}{2}\right)}{\sqrt{\sin\alpha}}\left(\frac{1-\cos\alpha}{1-\nu}-4\right)\right]_{\tan^{-1}(H^+/\Delta l)}^{\pi-\theta_f^+}. \tag{A3}$$

Similarly, along the bottom wake boundary, we obtain

$$\Delta K_-^{(2)} = \frac{Y\varepsilon_c\sqrt{H^-}}{2\sqrt{2\pi}(1+\nu)}\left[\frac{\cos\left(2\phi+\frac{\alpha}{2}\right)}{\sqrt{\sin\alpha}}\left(\frac{1-\cos\alpha}{1-\nu}-4\right)\right]_{\tan^{-1}(H^-/\Delta l)}^{\pi+\theta_f^-}. \tag{A4}$$

Combining eqns (A1), (A3) and (A4) and taking the steady state limit, we derive

$$\lim_{H^\pm/\Delta l\to 0}\Delta K^{(1)}+\Delta K_+^{(2)}+\Delta K_-^{(2)} = \frac{\eta}{4\pi}\frac{K^2}{2-\frac{\sqrt{2E}}{E_c}A(\phi-\omega)}\left[\sin^2\theta\sin\left(2\phi+\frac{\theta}{2}\right)(4\nu-3+\cos\theta)\right]_{\theta_i^-}^{\theta_f^+} \tag{A5}$$

where the dimensionless parameter group η is defined in eqn (8). The expression (17) has been used in the above derivation.

We finally evaluate the contribution from the frontal switching boundary. Along which one has

$$\frac{d\Gamma}{\sqrt{R}}\begin{Bmatrix}n_1\\n_2\end{Bmatrix} = \frac{d\theta}{\sqrt{2\pi}}\frac{K^2\varepsilon_c}{P_s E_c\left(2-\frac{\sqrt{2E}}{E_c}A(\phi-\omega)\right)}\begin{Bmatrix}3\sin\theta\sin\left(2\phi+\frac{5}{2}\theta\right)\\ \sin\left(2\phi+\frac{3}{2}\theta\right)-3\cos\theta\sin\left(2\phi+\frac{5}{2}\theta\right)\end{Bmatrix}. \tag{A6}$$

Substituting eqns (A6) and (21) into eqn (20) and integrating from θ_f^- to θ_i^-, and then from θ_i^+ to θ_f^+, one obtains

$$\Delta K^{(3)} = -\frac{\eta}{4\pi}\frac{K^{*}}{2-\frac{\sqrt{2E}}{E_c}A(\phi-\omega)}\left\{(1-\nu)[\sin(4\phi+3\theta)-\sin(4\phi+\theta)-\sin 2\theta]\right.$$

$$+\frac{3}{16}\sin(4\phi+2\theta)-\frac{5}{16}\sin(4\phi+4\theta)+\frac{1}{16}\sin(4\phi+6\theta)+\frac{1}{4}\sin(4\phi+\theta)$$

$$\left.-\frac{1}{4}\sin(4\phi+3\theta)+\frac{1}{2}\sin\theta+\frac{1}{4}\sin 2\theta\right\}_{\theta_i^-,\theta_i}^{\theta_i^+,\theta_i}. \quad \text{(A7)}$$

From eqn (15), it is straightforward to verify that the quantity in the curved brackets of eqn (A7) assumes the same values for $\theta = \theta_i^-$ and for $\theta = \theta_i^+$, so that the contributions from initial angles cancel out. Combining the remaining part of eqn (A7) with eqn (A5), one obtains

$$\Delta K = -\frac{\eta K^{*}}{2-\frac{\sqrt{2E}}{E_c}A(\phi-\omega)}[F(\phi)+(1-\nu)D(\phi)]. \quad \text{(A8)}$$

The D term is given by

$$D = \frac{1}{\pi}\left\{\sin\theta\sin\left(2\phi+\frac{\theta}{2}\right)\left[\sin\theta-\sin\left(2\phi+\frac{3}{2}\theta\right)\right]\right\}_{\theta_i}^{\theta_i^+} = 0. \quad \text{(A9)}$$

The last equality is derived by using eqn (16). Also be eqn (16), the F term in eqn (A8) can be evaluated as

$$F = \frac{1}{16\pi}\left\{\sin\theta\left[\frac{1}{4}-3\sin^2\theta-\cos\left(2\phi-\frac{3\theta}{2}\right)\right]\right\}_{\theta_i}^{\theta_i^+}. \quad \text{(A10)}$$

The function $F(\phi)$ has the periodicity relations listed in eqn (23). Furthermore, the combination of eqns (A10) and (16) will lead to the result of eqn (24).